

Comparative Study on Grinding Behavior of C-Face and Si-Face in Laser-Sliced 4H-SiC Wafers

Bixue Li^{1,a}, Xing Zhang^{1,b}, Qiu Chen^{1,c}, Linlin Che^{1,d}, Jianfei Zhang^{1,e},
Haoyu Fan^{1,f}, Xiangang Xu^{1,g}, Rongkun Wang^{1,h*}, Xiufang Chen^{1,i*}

¹State Key Laboratory of Crystal Materials, Institute of Novel Semiconductors, Shandong University, Jinan 250100, China

^alibx@mail.sdu.edu.cn, ^b17731872242@163.com, ^cchenqiu0629@sdu.edu.cn,
^d202214075@mail.sdu.edu.cn, ^ezjf2531@163.com, ^ffanhaoyu2001@163.com, ^gxxu@sdu.edu.cn,
^hwrk@sdu.edu.cn, ⁱcxf@sdu.edu.cn

Keywords: laser slicing, nanoindentation, precision grinding, silicon carbide.

Abstract. With the growing application of wide-bandgap semiconductors such as SiC in power electronics, efficient and low-damage machining of large-diameter, high-quality 4H-SiC wafers has become a critical research priority. This study systematically compares the grinding behavior of the C- and Si-faces of laser-sliced 4H-SiC wafers and reveals the effect of crystallographic anisotropy on tool wear. In the experiments, a picosecond laser was used to induce internal crystal modification, and multiple pairs of 12-inch high-purity semi-insulating crystals and wafers were obtained through ultrasonic separation. These wafers were subsequently ground using #800/#8000 resin-bonded diamond wheels. Material removal and wheel wear were recorded in real time, and the wheel wear ratio (W/M) was adopted as the key evaluation metric. Nanoindentation and white-light interferometry were further employed to characterize the mechanical properties and surface morphology of the two crystal faces. Results show that in both rough and fine grinding, the C-face demonstrates superior material removal performance despite its higher hardness, whereas the Si-face is more prone to wheel degradation. For thin wafers, residual laser focus near the surface further aggravates wheel wear. These findings establish a link between crystallographic anisotropy, laser-modified layer position, and wheel wear behavior, providing an experimental foundation for clarifying the underlying mechanisms and developing face-specific grinding strategies for high-quality SiC wafer fabrication.

Introduction

With the rapid development of next-generation power electronics, wide-bandgap semiconductors such as silicon carbide (SiC) have become essential materials for high-performance devices, enabling applications in electric vehicles, renewable energy systems, 5G communications, and aerospace electronics. Among them, 4H-SiC stands out due to its wide bandgap, high critical electric field, superior thermal conductivity, and excellent chemical stability. These properties offer significant advantages under high-power, high-frequency, and high-temperature conditions, positioning 4H-SiC as a promising alternative to conventional silicon-based devices. Consequently, the demand for high-quality, large-diameter SiC wafers has grown rapidly, highlighting the need for efficient and low-damage processing technologies.

Although diamond wire sawing is widely used for SiC wafer preparation, it suffers from excessive kerf loss and low processing efficiency, which increase costs and limit wafer quality^[1]. In contrast, laser-induced modification and slicing technologies enable high-precision wafer separation by inducing localized modifications within the crystal through nonlinear absorption^[2-7]. Nevertheless, laser-sliced wafers often exhibit kerf marks and heat-affected zones, necessitating subsequent precision grinding. By integrating these two processes, laser slicing not only significantly reduces material loss but also enables low-damage wafer preparation while maintaining high processing efficiency.

However, grinding, as a necessary process for removing the surface damage layer after laser slicing, still faces challenges. The anisotropy of 4H-SiC leads to significant differences in

mechanical responses under different crystallographic orientations. The carbon end (C-face) and the silicon end (Si-face) differ in hardness, elastic modulus and fracture toughness, which directly affect crack initiation, plastic deformation, dislocation structures and material removal mechanisms. In recent years, several scholars have investigated the material removal mechanisms of 4H-SiC with different orientations^[8-10]. Other studies have also reported that crystal orientation influences the wear and micro-chipping of diamond tools. However, these studies have mostly focused on nanoscale or small-scale simulations, and lacks systematic investigations of wafer-scale grinding behavior after laser slicing. At the same time, some studies have primarily focused on surface quality indicators such as roughness and subsurface damage^[11], while insufficient attention has been given to the quantitative correlation between grinding wheel wear and crystal orientation. This gap constrains the development of differentiated grinding strategies.

Therefore, a comparative investigation of the grinding behavior between the C-face and Si-face of laser-sliced 4H-SiC wafers is of great importance. Such a study not only enhances the understanding of how crystallographic anisotropy influences tool wear and material removal mechanisms, but also provides an experimental foundation for optimizing face-specific grinding parameters, thereby reducing wheel wear, improving machining efficiency, and extending tool life. In this work, C-face and Si-face wafers prepared by laser slicing are systematically compared in terms of material removal thickness, grinding wheel wear ratio, and surface morphology. The objective is to elucidate face-dependent grinding mechanisms and to offer guidance for the optimized manufacturing of high-quality 4H-SiC wafers.

Experimental Methods

Sample Preparation.

A 12-inch high-purity 4H-SiC single crystal was sliced using a picosecond laser operated at a wavelength of 1030 nm, a pulse width of 15 ps, and a maximum output power of 40 W. During slicing, the crystal was fixed on a five-axis precision motion platform with a ceramic vacuum chuck to ensure stability and positioning accuracy. Laser scanning was performed along a predefined trajectory perpendicular to the $(11\bar{2}0)$ crystal plane, with a scanning pitch of 200 μm . The target wafer thickness was 700 ± 20 μm . After laser modification, ultrasonic-assisted separation was employed to detach the wafers near the incident surface from the parent crystal, yielding complete thin-sheet structures.

Grinding Experiments.

The separated crystal-wafer pairs were ground using a grinding machine developed by the China Electronics Technology Group Corporation (CETC). Resin-bonded diamond grinding wheels (ZZSM) with grit sizes of #800 and #8000 were employed for rough and fine grinding, respectively. The overall process flow is illustrated in Figure 1. For grinding wheels of the same grit size, identical procedures were applied, with precise control of grinding depth to remove the laser-modified layer and residual slicing marks. Simultaneously, the material removal thickness and grinding wheel wear were recorded in real time, enabling direct comparison between the C-face and Si-face. To quantitatively evaluate tool degradation, the wheel wear ratio (W/M) was adopted as the primary metric, defined as the ratio of wheel wear to material removal. Both wafer removal thickness and wheel wear were automatically measured by the thinning machine with an accuracy of ± 1 μm .

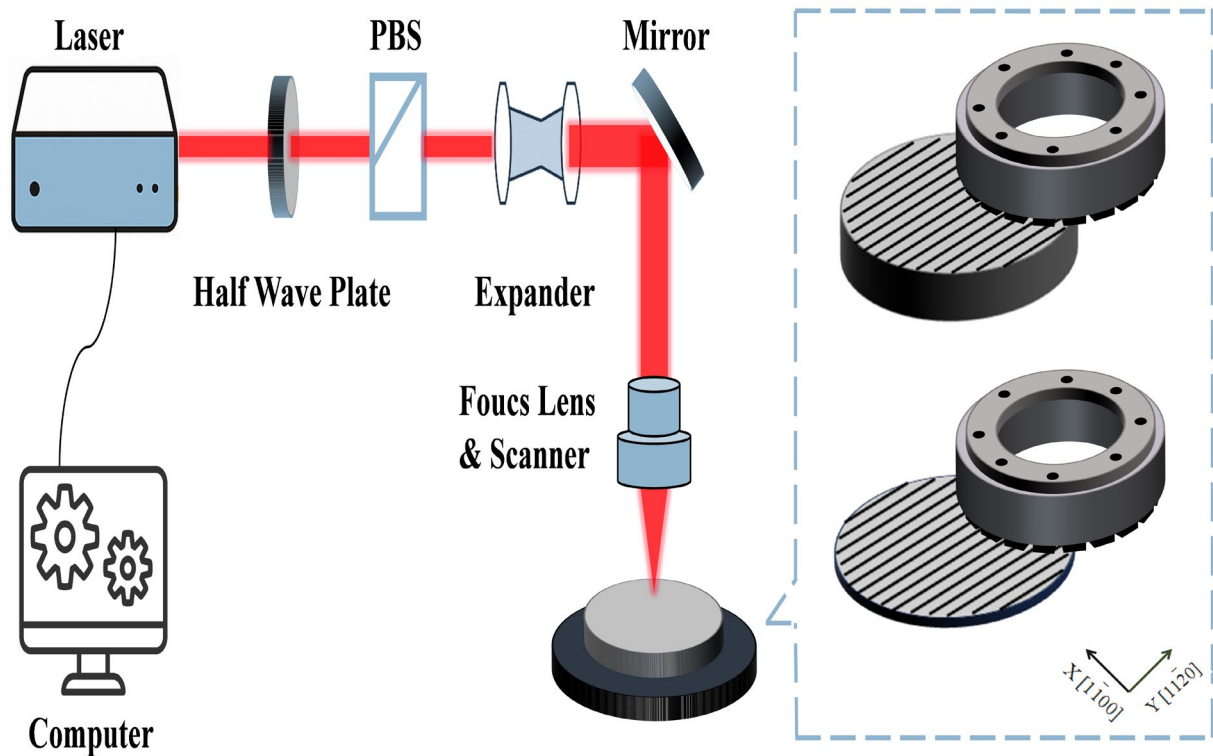


Fig. 1. Schematic of laser slicing and subsequent grinding applied to 4H-SiC wafers.

Characterization.

To evaluate the mechanical responses and machining quality of the C-face and Si-face, a KLA nanoindentation system was employed to measure the mechanical properties of polished 4H-SiC samples ($R_a < 5$ nm). A three-sided pyramidal Berkovich indenter was used in continuous stiffness measurement mode, and hardness (H) was extracted from the load–displacement curves. Surface topography and morphology were further characterized using a white-light interferometer (Sneox 090, Sensofar).

Results and Discussion

Nanoindentation Testing.

Multi-point nanoindentation tests were conducted on the C-face and Si-face of a high-purity 4H-SiC sample. The corresponding hardness–displacement into surface curves are presented in Figure 2. As shown, the hardness exhibits a rapid increase during the initial loading stage (0–50 nm), primarily due to surface roughness and residual surface stress^[12]. With further indentation (approximately 100–200 nm), the curves gradually stabilize and enter a plateau region. Statistical analysis within the stable range (300–350 nm) indicates that the average hardness of the C-face is approximately 44.21 ± 0.68 GPa, whereas that of the Si-face is approximately 41.34 ± 0.91 GPa. These values are consistent with the theoretical hardness^[13] of 4H-SiC reported in the literature^[13]. A direct comparison confirms that the C-face exhibits higher hardness than the Si-face.

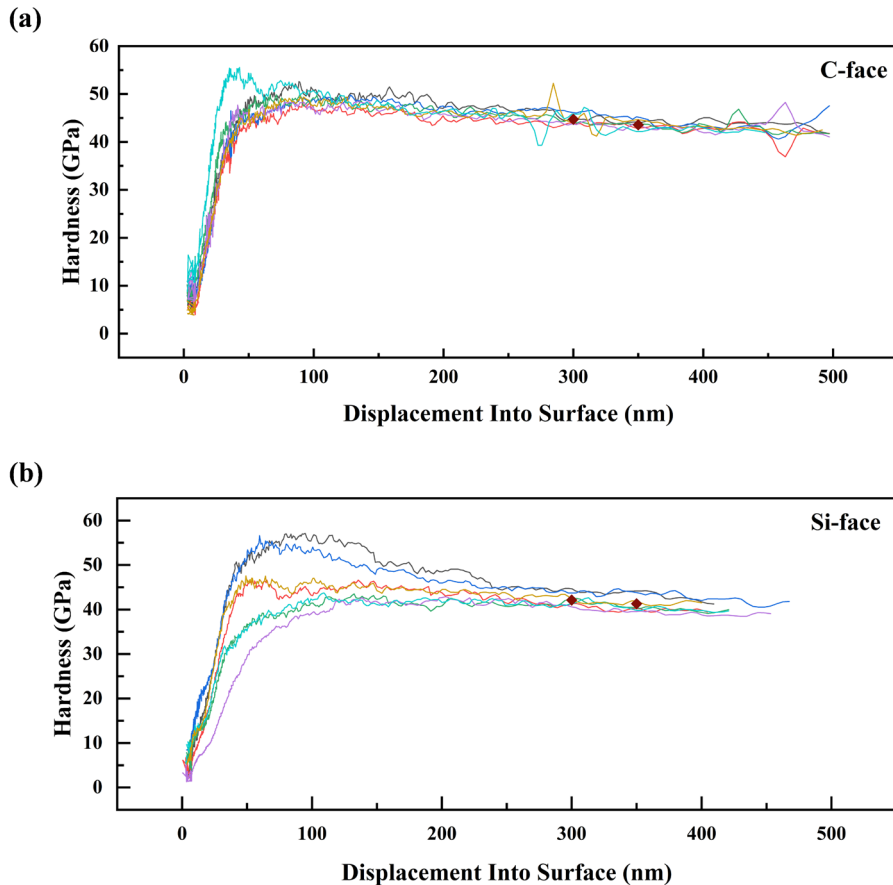


Fig. 2. Hardness measurement results: (a) Hardness of the C-face; (b) Hardness of the Si-face.

Effect of Crystal Plane Orientation on Wheel Wear Ratio.

During the rough grinding stage, distinct laser modification marks were observed on both the C- and Si-faces. After rough grinding, both faces gradually transitioned to flat regions, and by the completion of fine grinding, they exhibited uniform and smooth morphologies. Figure 3 presents the surface morphology evolution of the Si-face of a 4H-SiC wafer at different processing stages. Given the similar morphological evolution trends observed on both crystal faces, the Si-face is selected as a representative example to illustrate the typical surface morphology changes of laser-sliced wafers during rough and fine grinding.

As shown in Figure 4, under grinding wheels with different grit sizes, the wheel wear ratio of the C-face was consistently lower than that of the Si-face in both the rough and fine grinding stages, indicating that the Si-face is more susceptible to wheel degradation during grinding. Previous studies have also reported that although the C-face exhibits higher hardness and lower fracture toughness, its higher dislocation density facilitates stress release, thereby resulting in more favorable material removal behavior. In contrast, although the Si-face exhibits a slightly lower hardness than the C-face, its crystallographic orientation may to some extent restrict dislocation activity and weaken stress relaxation through dislocation slip during grinding, thereby promoting local stress accumulation and intermittent brittle removal events^[10]. This relatively single-dominant removal mechanism lacks the buffering effect of cooperative deformation modes, causing diamond abrasives and the bond to be continuously subjected to high local mechanical loading and frictional work. As a result, grit micro-crack propagation and bond degradation are accelerated, ultimately leading to an increased wheel wear ratio.

A further comparison between the rough and fine grinding stages reveals that the difference in wear ratio between the two faces is much greater during rough grinding than during fine grinding. This phenomenon arises not only from differences in crystal surface hardness but is also closely

related to the focal position in the laser slicing process. For laser sliced wafers, the laser focus typically resides near the upper wafer surface (Figure 5), making the Si-face more susceptible to grinding-induced wheel wear in subsequent processes, and consequently leading to a significant increase in its wear ratio.

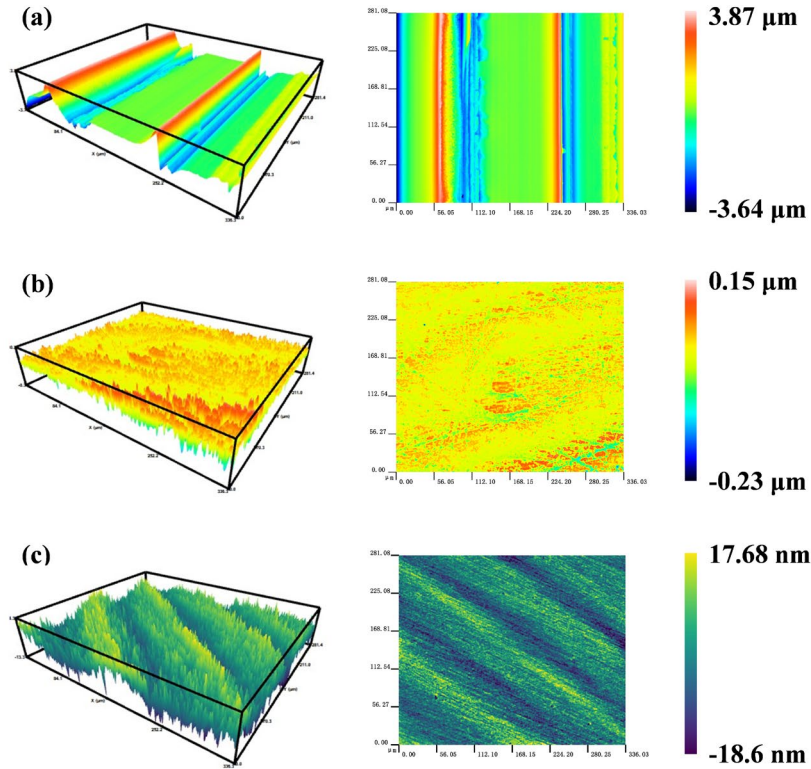


Fig. 3. Surface morphologies of the Si-face of 4H-SiC wafers: (a) as-received surface; (b) after grinding with #800 diamond wheel; (c) after fine grinding with #8000 diamond wheel.

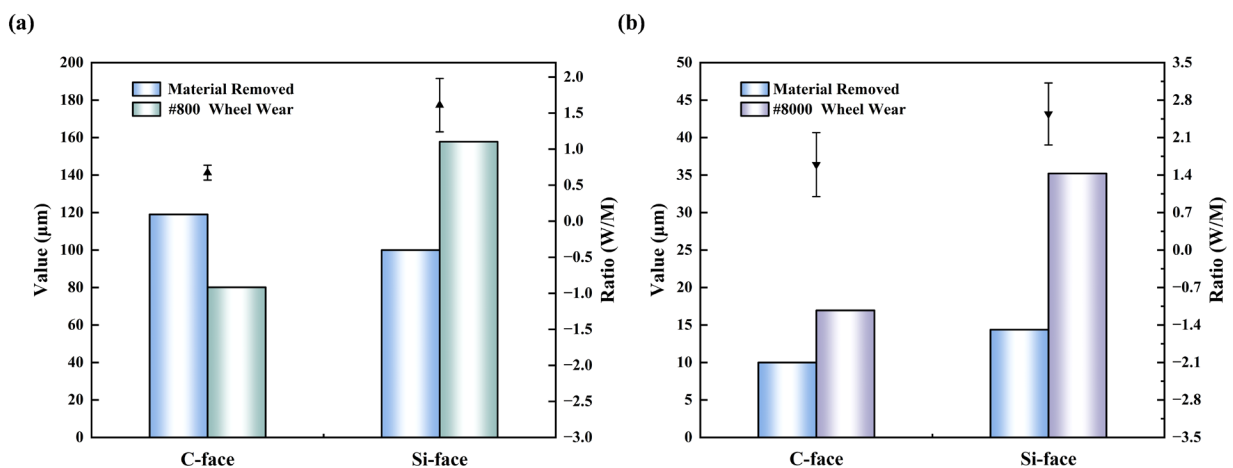


Fig. 4. Comparison of grinding performance between the C-face and Si-face: (a) material removal thickness, wheel wear, and wheel wear ratio during #800 rough grinding; (b) material removal thickness, wheel wear, and wheel wear ratio during #8000 fine grinding. The triangular symbols (▲) and error bars represent the wheel wear ratio (W/M), defined as the ratio of wheel wear to material removal.

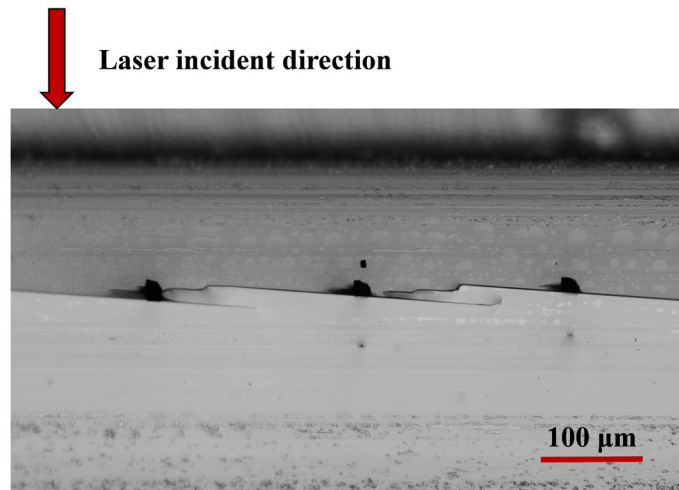


Fig. 5. Cross-sectional morphology of the 4H-SiC wafer after laser modification.

Summary

This study systematically compares the grinding behavior of the C- and Si-faces in laser-sliced 4H-SiC wafers. The results reveal pronounced differences in material removal and wheel wear. Under identical grinding conditions, the Si-face exhibits a higher wheel wear ratio. This behavior is closely related to the intrinsic anisotropy of 4H-SiC: the C-face possesses higher hardness and distinct fracture characteristics, while its higher dislocation density facilitates stress release, thereby reducing tool wear. In contrast, the Si-face displays a relatively single-dominant removal mechanism, which leads to increased wheel wear. Moreover, for thin wafers obtained by laser slicing, the focal position of the laser strongly influences subsequent grinding performance. When the focus remains near the wafer surface, the wear ratio of the Si-face increases significantly.

These findings provide valuable insights for optimizing SiC wafer grinding processes. Future work will integrate nanoindentation experiments with micro-cutting simulations to further elucidate the differences in mechanical response and crack evolution between crystal planes. In addition, the coupling between the laser-modified layer and subsequent grinding will be investigated to better elucidate the removal mechanisms of different crystallographic orientations, ultimately guiding the development of efficient processes for fabricating large-diameter, high-quality 4H-SiC wafers.

Acknowledgements

This work was supported by the National Natural Science Foundation of China (Grant No. U23A20569), the National Natural Science Foundation of China (62305189), the Key R&D Program of Shandong Province, China (2022ZLGX02) and Shandong Provincial Natural Science Foundation, China (ZR2022QF129).

References

- [1] M. Zou, F. Dou, Review of silicon carbide wafer cutting methods, *Superhard Mater. Eng.* 34 (2022) 35–41. (in Chinese).
- [2] E. Kim, Y. Shimotsuma, M. Sakakura, et al., Ultrashort pulse laser slicing of semiconductor crystal, *Proc. Pac. Rim Laser Damage 2016: Opt. Mater. High-Power Lasers* 9983 (2016) 40–45.
- [3] E. Kim, Y. Shimotsuma, M. Sakakura, et al., 4H-SiC wafer slicing by using femtosecond laser double-pulses, *Opt. Mater. Express* 7 (2017) 2450–2460.

-
- [4] K. Hirata, New laser slicing technology named KABRA process enables high speed and high efficiency SiC slicing, *Laser-Based Micro-and Nanoprocessing XII* 10520 (2018) 1052003.
- [5] M. Swoboda, R. Rieske, C. Beyer, et al., Cold split kerf-free wafering results for doped 4H-SiC boules, *Mater. Sci. Forum* 963 (2019) 10–13.
- [6] Y. Yao, Q. Chen, B. Li, et al., Influence of crystal orientation and incident plane on n-type 4H-SiC wafer slicing by using picosecond laser, *Opt. Laser Technol.* 182 (2025) 112174.
- [7] Q. Chen, Y. Yao, J. Zhang, et al., Effect of nitrogen doping concentration on 4H-SiC laser slicing, *J. Am. Ceram. Soc.* (2025) e20555.
- [8] Z. Tian, X. Chen, X. Xu, Molecular dynamics simulation of material removal mechanism during scratching of 4H-SiC and 6H-SiC, *Extreme Manuf.* 2 (2020) 045104. (in Chinese).
- [9] K. Tang, W. Ou, C. Mao, et al., Material removal characteristics of single-crystal 4H-SiC based on varied-load nanoscratch tests, *Chin. J. Mech. Eng.* 36 (2023) 111.
- [10] H. Wang, Z. Dong, R. Kang, et al., Surface characteristics and material removal mechanisms during nanogrinding on C-face and Si-face of 4H-SiC crystals: Experimental and molecular dynamics insights, *Appl. Surf. Sci.* 665 (2024) 160293.
- [11] J. Xia, Q. Yan, J. Pan, et al., Mechanism analysis and process optimization of nanogrinding single-crystal SiC, *Mater. Sci. Semicond. Process.* 175 (2024) 108218.
- [12] J. Cui, X. Yang, Y. Li, et al., Study on ultraprecision cutting characteristics of single-crystal silicon based on nanoindentation and nanoscratch experiments, *J. Synth. Cryst.* 52 (2023). (in Chinese).
- [13] K.E. Prasad, K.T. Ramesh, Hardness and mechanical anisotropy of hexagonal SiC single crystal polytypes, *J. Alloys Compd.* 770 (2019) 158–165.